

Supporting Information

Photoinduced Symmetry–Breaking Intramolecular Charge Transfer in a Quadrupolar Pyridinium Derivative

Benedetta Carlotti,^{*a} Enrico Benassi,^{*b} Anna Spalletti,^a Cosimo G. Fortuna,^c Fausto Elisei,^a
Vincenzo Barone^b

^a Department of Chemistry and Centro di Eccellenza sui Materiali Innovativi Nanostrutturati (CEMIN) University of Perugia, via Elce di Sotto 8, 06123 Perugia (Italy); ^b Scuola Normale Superiore, Collegio D'Ancona, via Consoli del Mare 15, 56126 Pisa (Italy); ^c Department of Chemical Sciences University of Catania, viale Andrea Doria 6, 95125 Catania (Italy).

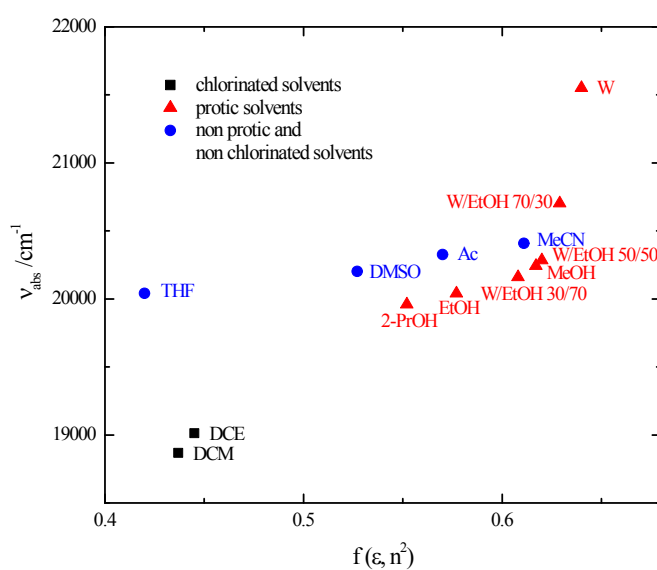


Figure S1. Solvatochromic shift of the absorption maximum of **2** as a function of solvent polarity.

Table S1. Cartesian components of the electric dipole moment μ (in D) and of the traceless electric quadrupole moment Θ (in D \cdot Å) for the ground state $|S_0\rangle$, the vertical Franck-Condon state $|S_{1v}\rangle$ and the relaxed first singlet excited state $|S_{1r}\rangle$, in DCM and in MeCN.

	DCM			MeCN		
	$ S_0\rangle$	$ S_{1v}\rangle$	$ S_{1r}\rangle$	$ S_1\rangle$	$ S_{1v}\rangle$	$ S_{1r}\rangle$
μ_x	-0.0001	0.0004	0.0002	0.0000	0.0010	6.8990
μ_y	-0.9132	-4.1721	-1.1436	-0.8423	-4.1725	-0.1107
μ_z	0.0424	-0.2572	0.2397	0.0727	-0.2570	-0.9654
μ	0.9142	4.1800	1.1685	0.8454	4.1804	6.9671
Θ_{xx}	136.5016	187.7428	139.1337	133.9498	189.3927	122.9859
Θ_{xy}	-0.0001	-0.0005	-0.0004	-0.0004	-0.0014	-1.4118
Θ_{xz}	-0.0008	-0.0009	0.0006	-0.0011	-0.0020	3.0397
Θ_{yy}	-45.5095	-73.0785	-44.6405	-44.0554	-74.1670	-45.3886
Θ_{yz}	-3.2637	-4.5006	0.3019	-3.2992	-4.5002	2.4756
Θ_{zz}	-90.9921	-114.6643	-94.4932	-89.8944	-115.2258	-77.5973

Solvatochromic shifts (see references: (a) P. Suppan and N. Ghoneim, “Solvatochromism”, The Royal Society of Chemistry, London, 1997, and references therein; (b) J. Lawokicz, “Principles of Fluorescence Spectroscopy”, Springer, New York, 2006; (c) I. Baraldi, “La luminescenza. Elementi di fotofisica molecolare”, Bononia University Press, Bologna, 2007, and references therein.)

The following discussion is a tentative rationalisation of the absorption solvatochromism of compound **2** because of the complexity of the system. This treatment gives just an indication of the two main contributions (monopole and quadrupole) probably determining the spectral shifts, as stated in the manuscript.

Three types of electric interactions among a solute and the solvent exist: (a) dispersion interactions, (b) interactions due to the transition multipole moments (normally truncated to the transition dipole contribution), and (c) multipolar interactions. In our elaboration, the formers have not been taken into account, since in the literature their role and reasonable description is still under discussion. The effect of an electric field on a non-polar polarisable molecule is defined as induction polarisation (*i*), whereas the corresponding effect on a rigid dipole is defined as orientation polarisation (*o*). The induction effects typically occur in shorter times with respect to the orientation effects. If two solvents are considered (namely 1 and 2) the contribution of the terms (b) and (c) to the energy variation due to the solvent change can be described according to the models deriving from Onsager’s treatment of the molecule inside a spherical cavity. The expressions for the induction and orientation contributions due to the transition dipole moment **M** are, respectively:

$$\Delta E_{1-2}(M) = -\frac{k_0}{2a^3} M^2 \Delta [f(n^2)]_{1-2}, \quad (i)$$

$$\Delta E_{1-2}(M) = -\frac{k_0}{2a^3} M^2 \Delta [f(\varepsilon) - f(n^2)]_{1-2}. \quad (o)$$

where $f(x)$ is the polarisation function, ε is the relative dielectric constant of the medium, n is the refractive index of the medium (all quantities are in SI units), $k_0 \equiv \frac{1}{4\pi\varepsilon_0}$, and a is the *radius* of the spherical cavity (according to Onsager’s

model). In the case of the multipolar interactions, the solvent is usually still treated as a dipole, whereas for our specific case of solute, the multipolar terms need to be considered up to the quadrupole. Therefore, the following contributions need to be taken into account: i) charge (solute)-dipole (solvent), described by the Born model; ii) dipole (solute)-dipole (solvent), described by Lippert-Mataga or McRae model; iii) quadrupole (solute)-dipole (solvent), described by Suppan-Ghoneim model:

$$i. \quad \Delta E_{1-2}(q) = -\frac{k_0}{2a} q^2 \Delta [F(n^2)]_{1-2}, \quad (i)$$

$$\Delta E_{1-2}(q) = -\frac{k_0}{2a} q^2 \Delta [F(\varepsilon) - F(n^2)]_{1-2}; \quad (o)$$

$$ii. \quad \Delta E_{1-2}(\mu) = -\frac{k_0}{2a^3} (\mu_e^2 - \mu_g^2) \Delta [f(n^2)]_{1-2}, \quad (i)$$

$$\Delta E_{1-2}(\mu) = -\frac{k_0}{a^3} \mu_g \cdot (\mu_e - \mu_g) \Delta [f(\varepsilon) - f(n^2)]_{1-2}; \quad (o)$$

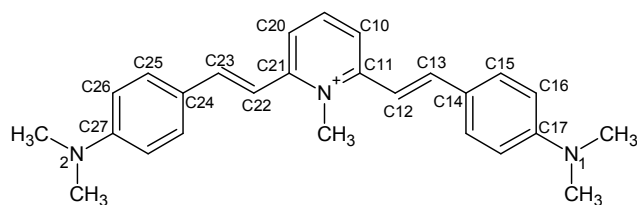
$$iii. \quad \Delta E_{1-2}(\Theta) = -\frac{k_0}{a^5} (\Theta_e^2 - \Theta_g^2) \Delta [f(n^2)]_{1-2}, \quad (i)$$

$$\Delta E_{1-2}(\Theta) = -\frac{k_0}{2a^5} \Theta_g (\Theta_e - \Theta_g) \Delta [f(\varepsilon) - f(n^2)]_{1-2}. \quad (o)$$

where the polarisation function $f(x) \equiv \frac{x-1}{2x+1}$ (when the solute dipole is considered non-polarisable, such as in Lippert-Mataga model) or $f(x) \equiv 2\frac{x-1}{x+2}$ (when the solute dipole is considered polarisable, such as in the McRae model), and $F(x) \equiv 1 - \frac{1}{x}$, q is the electrical charge, μ is the electrical dipole moment, and Θ is the electrical quadrupole moment. The values of M , μ , Θ issuing from our quantum mechanical computations then lead for **2** to the solvatochromic shifts (with respect to CHCl_3) collected in Table S2, assuming the solute dipole non-polarisable). The values of μ_e and Θ_e refer to the ones calculated for the vertical adiabatic S_1 state. (We remind that within Suppan-Ghoneim model the quadrupole moment is treated as a scalar quantity, *i.e.* $\Theta \equiv 2qd^2 = 2\mu d$; this is true just in case of pure, that is linear and centro-symmetrical quadrupoles.) As a consequence in equations (ii) μ'_g and μ'_e correspond to the computed dipole moments only if the axis origin coincides with the centre of charge of the system (as occurs in our computation); in the general case, for a charged system, we should use $\mu'_g = \mu_g - Q\mathbf{r}$ and $\mu'_e = \mu_e - Q\mathbf{r}$, respectively, where \mathbf{r} is the vector which describe the displacement with respect to the centre of charge of the system. Even though the models used are rather simplified for such a complex molecular system like the one under investigation, a shift toward higher energy of the absorption transition is foreseen by these calculations in all the considered solvents ($\Delta E(\text{tot})$ positive), which are more polar than the reference CHCl_3 , when only the inductive contributions are considered. Only induction polarisation contributions are taken into account because generally the transition dipole moment interaction takes place in very short (instantaneous) times, then the orientation contribution is usually neglected when just the solvatochromism in absorption spectra is considered. The experimentally found hypsochromic shift of the absorption spectrum upon increasing solvent polarity is therefore rationalised considering the contribution of the monopole (solute)-solvent interaction and the non-negligible contribution due to the quadrupole (solute)-solvent interaction, whereas the contribution due to the dipole (solute)-solvent interaction is always negligible.

Table S2. Contributions to the solvatochromic shifts in the absorption transition of **2** in different solvents with respect to CHCl_3 , calculated in eV according to the equations mentioned in the text.

Solvent	$\Delta E(M)$		$\Delta E(q)$		$\Delta E(\mu)$		$\Delta E(\Theta)$		$\Delta E(\text{tot})$	
	(i)	(o)	(i)	(o)	(i)	(o)	(i)	(o)	(i)	(o)
Ac	0.0099	-0.0454	0.0756	-0.2708	0.0007	-0.0011	0.0424	-0.0405	0.1286	-0.3578
DMSO	0.0030	-0.0440	0.0235	-0.2515	0.0002	-0.0011	0.0133	-0.0399	0.0402	-0.3366
MeCN	0.0124	-0.0553	0.0912	-0.3150	0.0009	-0.0013	0.0553	-0.0510	0.1598	-0.4227
EtOH	0.0102	-0.0498	0.0746	-0.2863	0.0007	-0.0012	0.0451	-0.0459	0.1306	-0.3804
MeOH	0.0140	-0.0551	0.1073	-0.3286	0.0011	-0.0014	0.0638	-0.0520	0.1863	-0.4371



Scheme S1

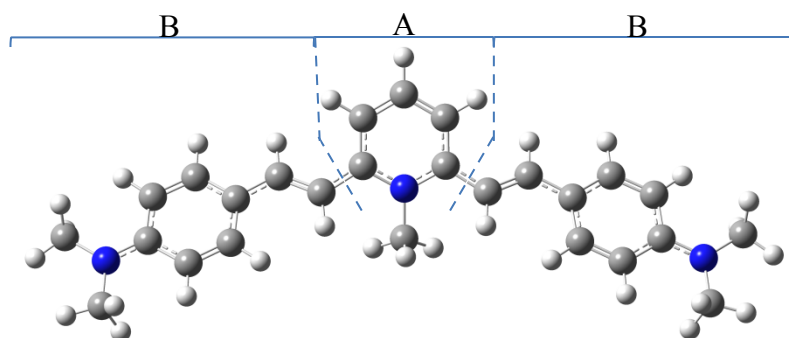
Table S3. Comparison between the dihedral angles δ (N, C11, C12, C13) and δ' (N, C21, C22, C23) for the S_0 and S_1 optimised geometries of **2** in DCM and MeCN. Values are reported in degrees.

	DCM		MeCN	
	δ	δ'	δ	δ'
S_1	163.4	160.4	108.1	178.5
S_0	157.5	157.5	146.7	147.2

Table S4. Comparison between $S_0 \rightarrow S_1$ and $S_0 \rightarrow S_2$ transitions: difference of electron density between states $\Delta\rho$ (in the figures the colour violet corresponds to an increase and the colour brown to a decrease in electron density, respectively), energy, oscillator strength and nature.

	DCM	MeCN
$S_0 \rightarrow S_1$		
$\Delta\rho_{01}$		
$\Delta E_{01} / \text{eV}$	2.3234	2.5307
f_{01}	1.7837	1.8857
nature	-0.17654 H- 2 \otimes L \rangle 0.23407 H- 1 \otimes L+ 1 \rangle 0.63076 H \otimes L \rangle	-0.17883 H- 2 \otimes L \rangle 0.23588 H- 1 \otimes L+ 1 \rangle 0.62918 H \otimes L \rangle
$S_0 \rightarrow S_2$		
$\Delta\rho_{02}$		
$\Delta E_{02} / \text{eV}$	2.6414	2.6545
f_{02}	0.3208	0.3339
nature	0.60023 H- 1 \otimes L \rangle 0.37051 H \otimes L+ 1 \rangle	0.58637 H- 1 \otimes L \rangle 0.39195 H \otimes L+ 1 \rangle

Table S5. Mulliken charge analysis of **2** in DCM and MeCN for the ground state $|S_0\rangle$, the vertical singlet excited states $|S_{1v}\rangle$ and $|S_{2v}\rangle$, the relaxed first singlet excited state $|S_{1r}\rangle$.

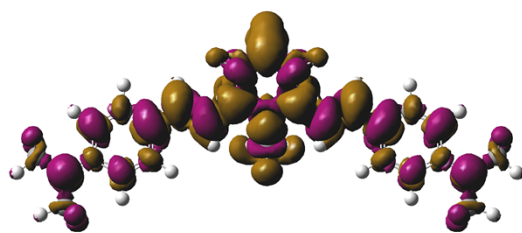


		S_0	S_{1v}	S_{1r}	S_{2v}
DCM	$Q(A) =$	0.2304	-0.0738	0.5580	-0.0237
	$Q(B) =$	0.3848	0.5369	0.2210	0.5118
MeCN	$Q(A) =$	0.2341	-0.0783	*	-0.0310
	$Q(B) =$	0.3829	0.5391		0.5155

*data not shown because of the symmetry broken optimised geometry of S_{1r} .

Table S6. Cartesian components of the electric dipole moment $\boldsymbol{\mu}$ (in D) and of the traceless electric quadrupole moment Θ (in D \cdot Å) for the $|S_{2v}\rangle$ state, in DCM and in MeCN.

	DCM	MeCN
	$ S_{2v}\rangle$	$ S_{2v}\rangle$
μ_x	0.0000	0.0000
μ_y	-3.7705	-3.8640
μ_z	-0.4909	-0.5010
μ	3.8023	3.8964
Θ_{xx}	178.6668	178.3629
Θ_{xy}	0.0000	0.0000
Θ_{xz}	0.0000	0.0000
Θ_{yy}	-70.1738	-69.9077
Θ_{yz}	-7.7408	-7.8678
Θ_{zz}	-108.4931	-108.4553



$\Delta\rho_{10}$ (DCM)

Figure S2. Difference of electron densities for the $S_1 \rightarrow S_0$ transition of **2** in DCM (the colour violet corresponds to an increase and the colour brown to a decrease in electron density, respectively).

Table S7. Excited states lifetimes and Species Associated Spectra (SAS, calculated by Target Analysis) of **1** in solvents of different polarity (obtained by transient absorption upon excitation at 400 nm): data from ref. 40.

Solvent	τ / ps	λ / nm
CHCl ₃	2.0	<625(-)
	26	560(-)
	79	590(-)
	rest	570(+)
DCM	0.70	<625(-)
	52	585(-)
	134	550(+), 605(-)
	rest	580(+)
DCE	0.96	<650(-)
	4.2	590(-)
	177	605(-)
	rest	575(+)
DMSO	0.20	525(-), 600(+)
	3.1	585(-)
	45	540(+), 625(-)
Ac	0.30	570(-)
	1.2	525(+), 605(-)
	28	540(+), 630(-)
MeCN	0.19	590(+)
	0.75	590(-)
	19	535(+), 625(-)
EtOH	0.78	540(-)
	10	580(-)
	52	535(+), 605(-)
MeOH	0.22	540(-)
	2.9	580(-)
	24	535(+), 620(-)
W/MeOH 90/10	0.81	580(-)
	6.7	520(+), 620(-)

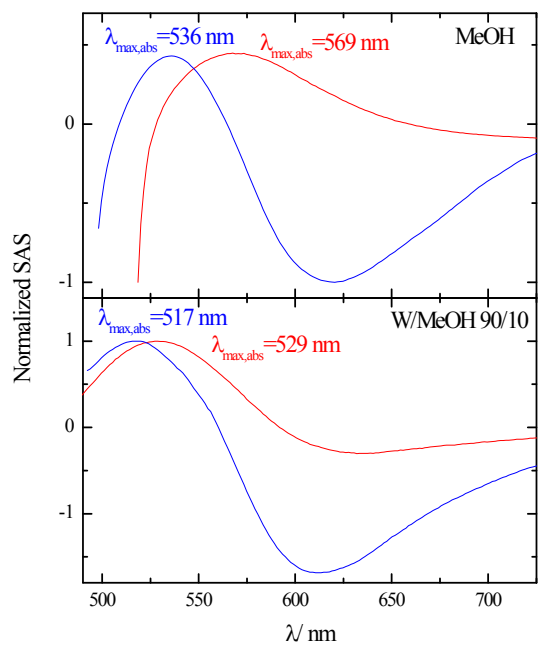


Figure S3. Normalised SAS spectra of the longer living component (the lowest excited singlet state with an ICT character) obtained for compound **1** (blue) and **2** (red) in MeOH (panel on top) and W/MeOH 90/10 (panel on bottom) obtained from the Target Analysis of the femtosecond transient absorption data.

Table S8. Simulated $S_1 \rightarrow S_n$ TD-DFT transition energies and wavelengths ($n = 2, 3, 4, 5$) of **2** in DCM and MeCN.

	DCM		MeCN	
	$\Delta E / \text{eV}$	λ / nm	$\Delta E / \text{eV}$	λ / nm
$n = 2$	2.1093	588	2.1793	569
3	2.5322	490	2.5292	490
4	2.8912	429	3.1608	392
5	2.9659	418	3.5545	349

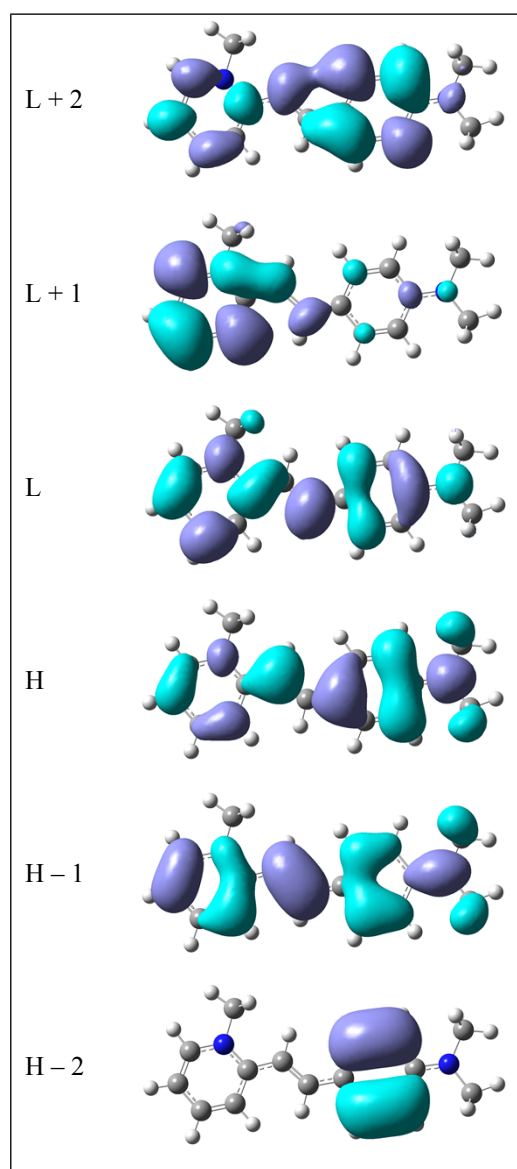


Figure S4. Frontier MOs for compound **1** in DCM.